Pergamon

Int. J. Heat Mass Transfer. Vol. 38, No. 12, pp. 2251–2258, 1995
Elsevier Science Ltd

0017-9310/95 $9.50+0.00

0017-9310(94)00354-8

Improvements to the discrete transfer method of calculating radiative heat transfer

P. S. CUMBER

British Gas plc, Research and Technology, Gas Research Centre, Ashby Road, Loughborough, Leicestershire LE11 3QU, U.K.

(*Received* 14 *March* 1994 *and in final form* 12 *October* 1994)

Abstract—In this article the discrete transfer method developed by Lockwood and Shah for calculating radiative heat transfer is examined. Various aspects of the algorithm are analysed and modifications suggested to improve the accuracy and computational performance. These modifications are evaluated by comparing predicted heat fluxes with analytic and numerically accurate solutions to test problems and measured fluxes from experiments. The evaluation study shows that the modifications yield significant improvements over the original algorithm.

1. INTRODUCTION

There are many applications where the accurate modelling of radiative heat transfer combined with other modes of heat transfer and fluid flow is important. One example of an application where thermal radiation is a dominant mode of heat transfer is the hazard analysis of fires in enclosures, in particular the prediction of flashover [1] and flame spread. Another application where there is a requirement to predict the radiative heat distribution is the safety analysis of flaring and venting operations. One final example of an application where the accurate modelling of radiation is beneficial is in the design of burners and furnaces where a primary objective is the minimisation of oxides of nitrogen (NO_x) emission, as NO_x production is highly sensitive to changes in the temperature field [2].

The modelling of thermal radiation together with the solution of the fluid dynamic equations [3] necessary to predict the fluid flow and heat transfer for a combusting system is a formidable task. In some scenarios the influence of radiative heat transfer on the fluid motion is small, with only small perturbations to the density field occurring. In this situation radiative heat transfer in the gas phase can be modelled using relatively crude models, see for example [4], or where the laminar flamelet combustion model is implemented, by introducing a heat loss to the flamelet library [5]. The radiation distribution incident to any surface of interest can then be calculated in an uncoupled fashion, once the fluid dynamic system of equations is converged, using a more sophisticated radiation model [5]. For the areas of application mentioned above; the prediction of flashover, flame-spread and NO_x production, radiation can have a large effect which requires accurate calculation of the radiative heat distribution and fluid flow in a coupled manner.

A number of numerical techniques exist for solving the equation governing the transfer of thermal radiation, examples being Hottel's zone method [6], Monte Carlo techniques [6] and flux models [7]. Each of the above methods have their advantages and disadvantages, a detailed discussion of which can be found in [7]. In this article the radiation model considered is the discrete transfer method developed by Lockwood and Shah [7]. This algorithm has similarities to all three numerical techniques mentioned above, harnessing the advantages of each without many of the disadvantages. The method is numerically exact, geometrically flexible and easily coupled to a computational fluid dynamics solver. The discrete transfer method can also be implemented easily with most emissivity models such as the mixed grey gas model [8], the total transmittance non-homogeneous model [9], exponential wide band models [10] and narrow band models [9]. One final consideration is that the discrete transfer method is ideal for implementing on parallel computer architectures. These attractive features have made the discrete transfer method a popular model with many groups interested in heat transfer applications [5, 11, 12].

The discrete transfer method of calculating radiative heat transfer involves the tracing of representative rays from one surface to another through the domain of interest. The intensity distribution along each ray is calculated by solving a discretisation of the equation of radiative heat transfer. Essentially the more rays traced, the more accurate the prediction of radiative heat distribution obtained. There are many situations where accurate prediction of radiative heat flux requires a large number of rays, particularly where the view factor from the high temperature emitting regions is small [5]. One further consideration is that tracing rays through the domain can be computationally expensive, especially for body fitted grids.

NOMENCLATURE

I	radiant intensity
K_a	absorption coefficient
L	path length
N_θ, N_ϕ	number of rays in the θ and ϕ directions
P, Q, R	points on the unit hemisphere
Q	quadrature formulae
q	heat flux
S_p	speed-up coefficient
s	distance co-ordinate
T	temperature
t_{cal}, t_{sto}	execution times
w_1, w_2	quadrature weights in Q_{Gauss}
x'	distance from stack.

Greek symbols

α_1, α_2, β_1	parameters in Q_{Gauss}
Δs	distance travelled by a ray in a control volume
$\Delta\Omega$	solid angle around Ω
$\Delta\theta$, $\Delta\phi$	ray mesh spacing in the θ and ϕ directions
ε	emissivity
Ω	ray direction
θ, ϕ	spherical co-ordinates
σ	Stefan–Boltzmann constant.

Subscripts

c	control volume centre
g	gas phase quantity
Gauss	a specific quadrature formula
i	number of rays (Fig. 6)
i, j	spherical co-ordinates of ray direction
Newt	a specific quadrature formula
n, $n+1$	entry and exit points of a ray traversing a control volume
new, old	current and previous iterations
Shah	quadrature formula used by Shah [13]
w	quantity associated with a wall
∞	numerically exact quantity.

Superscripts

$^-$	quantity incident to a wall.

In the following sections the numerical accuracy and computational efficiency of the discrete transfer method is analysed. Suggestions are made for improvements to the algorithm and finally these improvements are evaluated by comparing predicted heat fluxes with analytic and numerically accurate solutions to test problems and measured fluxes from experiments.

2. ASPECTS OF THE DISCRETE TRANSFER METHOD

A detailed description of the discrete transfer method can be found in Lockwood and Shah [5]. We will only consider aspects of the algorithm of relevance to the issues addressed in the present article.

In the discrete transfer method the domain of interest is overlaid with a computational mesh and representative rays are traced from one surface to another, through the intervening control volumes defined by the mesh. The transfer equation for thermal radiation along a ray, neglecting scattering can be expressed in the form,

$$\frac{dI}{ds} = -K_a I + \frac{K_a \sigma T^4}{\pi}. \quad (1)$$

For any representative ray the intensity distribution can be calculated by assuming each control volume is homogeneous. Under this assumption equation (1) can be integrated to give the recurrence relation

$$I_{n+1} = \frac{\sigma T_c^4}{\pi}(1 - e^{-K_a \Delta s}) + I_n e^{-K_a \Delta s} \quad (2)$$

where I_n and I_{n+1} are the intensity of the ray on entry and exit, respectively and Δs is the distance travelled in the control volume. Therefore, given the initial intensity at a point on an emitting surface, the change in intensity along the ray can be calculated using equation (2). The initial intensity is specified by taking the walls to be Lambert surfaces.

For grey walls the emitted intensity is dependent on the incident flux q^-

$$q^- = \int_{2\pi} I_w^-(\Omega) \cos\theta \, d\Omega \quad (3)$$

where I_w^- is the incident intensity. In the discrete transfer method the incident flux integral is replaced by a numerical quadrature

$$q^- = \Sigma I_w^-(\Omega) \cos\theta \Delta\Omega \quad (4)$$

The values of incident intensity I_w^- at a point on a wall are calculated by tracing rays from the point and backtracking from the walls intercepted, applying equation (2) through each control volume. Hence for grey walled enclosures the coupling between the incident flux and emitted intensity make the discrete transfer method a guess and correct procedure in which an estimate of the incident flux distribution is iteratively improved.

3. IMPROVEMENTS TO THE DISCRETE TRANSFER METHOD

The first aspect of the discrete transfer method considered is the numerical integration of the incident intensity field to calculate the incident flux.

3.1. *Quadrature formulae*

In the description of the discrete transfer method given above the discretisation of the hemisphere of incident intensity was not considered. One possible discretisation is a uniform distribution of rays on the surface of the hemisphere. This discretisation is the one used by Guilbert [14] but it is not clear that this is the optimum discretisation as Lambert's cosine law increases the significance of incident intensity for small azimuthal angles.

Rather than have a uniform distribution of rays on the hemispherical surface Shah [13] used a uniform distribution of rays in the spherical co-ordinates (θ, ϕ), that define the unit hemisphere. For more than four rays a nonuniform distribution of rays on the hemisphere surface is produced, with a finer mesh for small azimuthal angles. A further advantage of working explicitly with local spherical co-ordinates is more accurate quadrature formulae can be derived. Shah [13] derived the following quadrature formula by assuming the intensity distribution is constant in each element of the unit hemisphere, defined by the discretisation in (θ, ϕ) space

$$q^- = \sum_{j=1}^{N_\phi} \sum_{i=1}^{N_\theta} I_w^-(\theta_i, \phi_j) \cos\theta_i \sin\theta_i \sin\Delta\theta\, \Delta\phi. \quad (5)$$

For convenience this quadrature formula is labelled Q_{Shah}. This is not the only quadrature rule that can be derived in this way. Suppose the incident intensity is evaluated at the corners of each hemispherical element, and the incident intensity distribution has the form

$$I = \begin{cases} a+b\theta+c\theta\phi & 0 \leqslant \theta \leqslant \Delta\theta \\ a+b\theta+c\phi+d\theta\phi & \Delta\theta < \theta \end{cases}$$

where a, b, c and d are arbitrary, then the incident flux integral can be evaluated exactly.

One disadvantage of locating rays at the corners of hemispherical elements is that some rays are traced parallel to the surface. In practice this leads to poor results because of the $\cos\theta$ dependence and makes it inappropriate to use the composite quadrature formula, for one- and two-dimensional geometries, where surfaces in the redundant co-ordinate directions can be specified as perfect reflectors. To remove this difficulty the intensity distribution in hemispherical elements adjacent to the surface are assumed constant rather than bilinear. This gives the composite quadrature formula

$$q^- = I_w^-(0,0)\,\Delta\Omega_0 + \sum_{j=1}^{N_\phi} \sum_{i=1}^{N_\theta} I_w^-(\theta_i, \phi_j)\,\Delta\Omega_i$$

$$\Delta\Omega_i = \begin{cases} \dfrac{\pi}{2}\left(1 - \dfrac{\sin 2\Delta\theta}{\Delta\theta}\right) & i = 0 \\ \dfrac{\Delta\phi}{4}\left(\dfrac{\cos 2\theta_2 \sin\Delta\theta}{\Delta\theta} - \cos(2\theta_2 + \Delta\theta) + \dfrac{\sin 2\Delta\theta}{2\Delta\theta} - \cos 2\Delta\theta\right) & i = 1 \\ \dfrac{\Delta\phi}{4}\left(\dfrac{\cos 2\theta_{i+1} \sin\Delta\theta}{\Delta\theta} - \cos(2\theta_{i+1} + \Delta\theta) + \cos(2\theta_i - \Delta\theta) - \dfrac{\cos 2\theta_i \sin\Delta\theta}{\Delta\theta}\right) & i = 2, 3, \ldots, N_\theta - 2 \\ \dfrac{\Delta\phi}{4}\left(\cos(2\theta_{N_\theta - 1} - \Delta\theta) - \dfrac{\cos 2\theta_{N_\theta - 1} \sin\Delta\theta}{\Delta\theta}\right) & i = N_\theta - 1 \\ \Delta\phi \cos\theta_{N_\theta} \sin\theta_{N_\theta} \sin\Delta\theta & i = N_\theta \end{cases} \quad (6)$$

$$\theta_i = \begin{cases} i\Delta\theta & i = 0, 1, \ldots, N_\theta - 1 \\ (i - 0.5)\Delta\theta & i = N_\theta. \end{cases}$$

This quadrature formula has the same formal accuracy as equation (5) because of the constant intensity assumption for the hemispherical elements adjacent to the surface, but as $\Delta\phi$, $\Delta\theta$ are reduced it should be accurate for intensity distributions well approximated by piece-wise linear profiles. This quadrature formula is analogous to a Newton Cotes formula for numerical integration on an interval [15]. For future reference this quadrature formula is denoted Q_{Newt}.

It is possible to derive Gaussian type quadrature formulae [15], which are formally more accurate than Newton Cotes formulae for the same computational effort. However the only stable quadrature formula that can be derived can only be applied to hemispherical elements with corners located at (0,0), (π/2,0), (π/2,$\Delta\phi$) and has the form

$$Q = \Delta\phi\{w_1 I_P + w_2(I_Q + I_R)\}$$

where I_P, I_Q, I_R are the incident intensity at the points $P(\alpha_1\pi/2, \Delta\phi/2)$, $Q(\alpha_2\pi/2, (1-\beta_1)\Delta\phi/2)$ and $R(\alpha_2\pi/2, (1+\beta_1)\Delta\phi/2)$, respectively. The values of the parameters w_1, w_2, α_1, α_2 and β_1 to six significant figures are given in Table 1. For future reference this quadrature formula is labelled Q_{Gauss}. Q_{Gauss} integrates intensity distributions that are quadratic in ϕ and cubic in θ, exactly, however, it can only be used with relatively few rays as the hemispherical mesh can only be refined by reducing $\Delta\phi$. Q_{Gauss} should give accurate estimates of incident flux relative to the number of rays traced for large values of $\Delta\phi$, but as $\Delta\phi$ is reduced will not necessarily converge to the correct value.

In this section a number of quadrature formulae

Table 1. Parameters in the quadrature formula Q_{Gauss}

$w1$	$w2$	$\alpha 1$	$\alpha 2$	$\beta 1$
0.25	0.125	0.282382	0.717618	0.685412

have been derived for calculating the incident flux at a point from the incident intensity distribution. The other aspect of the discrete transfer method where a numerical approximation is used is the calculation of the change in intensity along rays passing through the participating media. It is this topic that is discussed further in the next section.

3.2. *Integrating the thermal radiation equation*

Recall the recurrence relation (2) for the intensity distribution along a representative ray was derived by assuming the absorption coefficient and the temperature were constant in each control volume traversed. The recurrence relation (2) provides a simple method for calculating the intensity leaving a control volume in a prescribed direction from quantities readily available. However, a more accurate recurrence relation can be derived by assuming the temperature varies linearly between the entry and exit points of a ray traversing a control volume. Integrating equation (1) using this assumption gives the recurrence relation,

$$I_{n+1} = \begin{cases} \left(I_n - \dfrac{\sigma}{\pi} f\left[T_n; \dfrac{\Delta T}{K_a \Delta s}\right]\right) e^{-K_a \Delta s} \\ \qquad + \dfrac{\sigma}{\pi} f\left[T_{n+1}; \dfrac{\Delta T}{K_a \Delta s}\right] & K_a > 0 \\ I_n & K_a = 0 \end{cases} \tag{7}$$

$$\Delta T = T_{n+1} - T_n$$

$$f[T; U] = T^4 - 4T^3 U + 12T^2 U^2 - 24TU^3 + 24U^4$$

where T_n and T_{n+1} are the temperature on entry and exit, respectively to the control volume. Using the recurrence relation (7) in the discrete transfer method coupled to a computational fluid dynamic solver introduces interpolation errors to the calculation of T_n and T_{n+1}, but the more accurate representation of the temperature field in the radiation calculation should give significant improvements in the accuracy of the intensity prediction, because of the nonlinear dependence of the intensity on the temperature.

4. EVALUATION OF THE DISCRETE TRANSFER METHOD

In this section the modifications to the discrete transfer method discussed above are evaluated by comparing predicted heat fluxes with analytic and numerically accurate solutions to test problems and measured fluxes. For each test problem the predictions using the suggested improvements to the algorithm are also compared with Shah's [13] original algorithm. Shah's original algorithm is defined to be the discrete transfer method incorporating the recurrence relation (2) and the quadrature formula Q_{Shah}.

4.1. *Radiative heat transfer between parallel surfaces*

For the case of a constant absorption coefficient Heaslet and Warming [16] derived equations for the temperature field and net radiative flux, for finite values of emissivity and zero radiative source. For this test problem the conditions at the two respective surfaces are $T_{w1} = 1000$ K, $\varepsilon_{w1} = 0.9$ and $T_{w2} = 300$ K, $\varepsilon_{w2} = 0.5$. For this grey-walled scenario the convergence criteria and the initial incident flux distribution used are respectively,

$$\frac{\Sigma |q^-_{\text{old}} - q^-_{\text{new}}|}{\Sigma q^-_{\text{new}}} < 0.01 \quad q^- = 0.$$

This problem is one-dimensional but is solved in a three-dimensional domain $[0, L] \times [0, L] \times [0, L]$ by specifying the surfaces in the redundant co-ordinate directions as perfect reflectors. A uniform grid of six control volumes in each co-ordinate direction is specified.

Figure 1 shows comparisons of exact dimensionless heat flux with predicted values, using four rays per

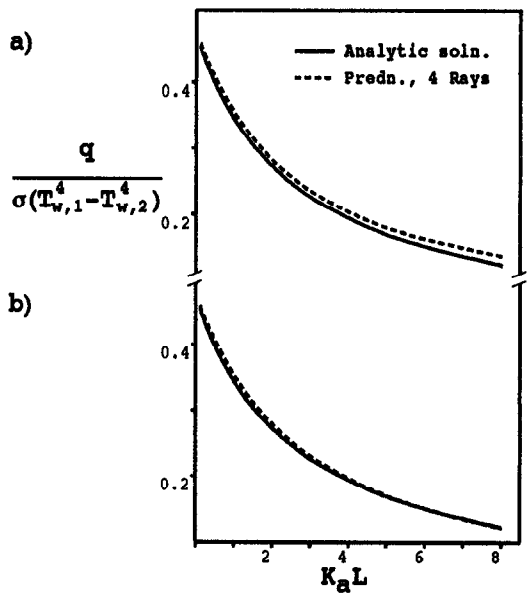

Fig. 1. Comparison of predicted fluxes with analytic solution for 1D problem. Predictions calculated using (a) Shah's original algorithm and (b) recurrence relation (7).

wall cell, for different values of optical thickness. Figure 1(a) shows the predicted heat flux using Shah's [13] original algorithm. The predicted heat flux is physically reasonable, with a monotone decrease in heat flux with increasing optical depth. However with increasing optical depth the error between the analytic and numerical solution increases. The trend in the error is due to the increased variation in the temperature field as the absorption coefficient is increased. Figure 1(b) shows the predicted heat flux calculated using the quadrature formula Q_{Shah} and the recurrence relation (7). The predicted heat flux is improved compared to the previous simulation, particularly for large values of optical thickness where the improved approximation of the temperature field is significant.

Applying the discrete transfer method to this geometrically simple problem with the quadrature formula Q_{Shah} and the recurrence relations (2) and (7) has made it possible to evaluate these numerical approximations. In the next two sections more geometrically challenging problems are considered to evaluate the quadrature formulae Q_{Newt} and Q_{Gauss}.

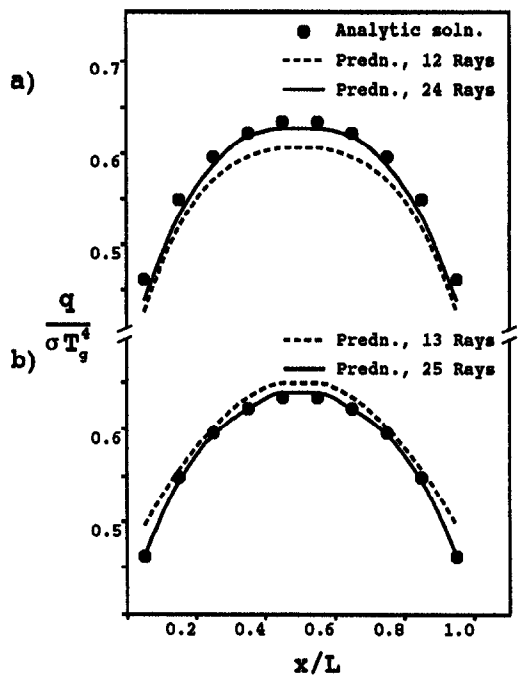

Fig. 2. Comparison of predicted fluxes with analytic solution for 2D duct. Predictions calculated using (a) Shah's original algorithm and (b) Q_{Newt} quadrature formula.

4.2. *Radiative heat transfer in a duct*

In this test problem, radiative heat transfer in a square cross-sectioned duct of infinite length is considered. The walls of the duct are cold and black. The interior of the duct is at a temperature $T_g = 1000$ K with an absorption coefficient $K_a = 1$. Under these conditions J. Gibb derived an analytic solution for the heat flux, which can be found in Shah [13].

For this two-dimensional problem a uniform grid of 10×10 control volumes is prescribed. In Fig. 2 predictions of dimensionless heat flux along one of the duct walls, normal to the length of the duct are compared with the analytic solution. Figure 2(a) is a comparison between the analytic solution and Shah's original algorithm with 12 and 24 rays per wall cell, whereas Fig. 2(b) is a comparison between predictions of heat flux using Q_{Newt} with 13 and 25 rays per wall cell to evaluate equation (3) with the analytic solution. Note the increased accuracy of Q_{Newt} compared to Q_{Shah} with nominally the same computational cost.

Predictions using the quadrature formula Q_{Gauss}, (not shown) are similar to Q_{Newt}. The disappointing performance of Q_{Gauss} for this problem is likely to be due to its relative simplicity, in the next section a more realistic scenario is considered.

4.3. *Radiative heat transfer in a furnace*

The test problem considered is one used previously by Shah [13] to demonstrate that the discrete transfer method is numerically exact. Shah [13] considered the scenario presented below to be representative of radiative heat transfer in a typical furnace. The furnace is cylindrical in shape with a radius of 1 m and length 5 m. The walls are at a temperature of $T_w = 500$ K with an emissivity of $\varepsilon_w = 0.8$. Within the furnace the conditions are,

$$T_g = 1700\,\text{K}, \quad K_a = 0.6\,\text{m}^{-1}$$
$$0 < r < 0.5 \quad 0 < z < 2.5$$
$$T_g = 1100\,\text{K}, \quad K_a = 0.05\,\text{m}^{-1}$$
otherwise.

A uniform mesh in each of the co-ordinate directions (r, z) is specified to give 4×20 control volumes. As the walls of the furnace are grey, the convergence criteria and the initial estimate of the incident flux specified for the one-dimensional problem discussed earlier are used. As one of the primary interests in this article is the rate of convergence of the heat flux distribution as the number of rays is increased, the predictions of heat flux distribution using relatively few rays are compared in Fig. 3 with a ray converged heat flux distribution using Shah's [13] original algorithm.

In Fig. 3(a) the predicted heat flux using Shah's [13] original algorithm with 12 and 24 rays is compared with the numerically accurate distribution. As can be seen both coarse ray predictions underpredict the numerically accurate prediction, although doubling the number of rays improves the agreement. Figure 3(b) is similar to Fig. 3(a) with the coarse ray predictions with 13 and 25 rays calculated using Q_{Newt} to evaluate the incident intensity integrals. Comparing the original algorithm's predictions with those calculated with Q_{Newt}, there is a significant improvement in accuracy using Q_{Newt}. The final figure in the series,

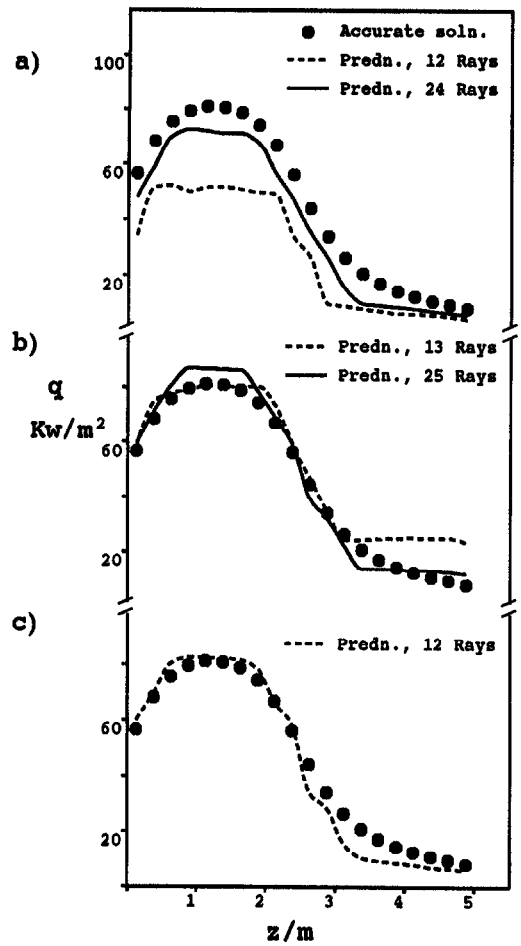

Fig. 3. Comparison of predicted fluxes with numerically accurate solution for furnace. Predictions calculated using (a) Shah's original algorithm, (b) Q_{Newt} quadrature formula and (c) Q_{Gauss} quadrature formula.

Fig. 3(c), is a comparison of the predicted heat flux distribution using Q_{Gauss} with 12 rays with the numerically accurate distribution. Of the predictions of heat flux using 12 and 13 rays, Q_{Gauss} is the superior. However as the number of rays is increased Q_{Gauss} does not converge to the correct heat flux distribution. This nonconvergence property as discussed previously makes this quadrature formula of academic interest only and will not be discussed further.

Although Shah [13] considered this scenario to be representative of radiative heat transfer in furnace applications, the step changes in the temperature field are physically unrealistic. In the final test problem considered below, a more realistic temperature field is prescribed making it possible to compare Shah's [13] original algorithm with a version of the discrete transfer method with Q_{Newt} and the recurrence relation (7) implemented.

4.4. *External radiation field from a flare*

The calculation of the external radiation field from a wind blown natural gas flare is a challenging problem. The flare issues from a stack 12 m above ground level with a diameter of 0.6 m, and a mass flow rate of 77 kg s^{-1} into a cross-wind of 4 m s^{-1} at 10 m above ground level. In the radiation calculations discussed below the flame structure is calculated from an integral model described in detail in Cook [17] and [18] and extensively validated in Cook [17, 18] and Caulfield *et al.* [19]. Briefly the integral model is a system of ordinary differential equations derived from the Reynolds equations [3] by imposing self similarity in the stream-wise direction, and prescribing empirical entrainment relations. The turbulence closure used is a one-dimensional k–ε model. The combustion process is modelled using a conserved scalar/prescribed probability density function approach using the laminar flamelet concept, extended to account for soot formation and consumption.

The flame structure is calculated in a curvilinear co-ordinate system (s, r), where s is the curvilinear distance along the trajectory of the flare and r is normal to s. To use this characterisation of the flame structure in the radiation calculations the temperature, soot and chemical composition predictions are interpolated on to a Cartesian grid, and a mixed grey gas model [8] applied to prescribe the absorption coefficient field. The origin of the Cartesian domain is taken to be the centre of the stack exit. Labelling the downwind direction x, cross-wind direction y and vertical direction z, there is a plane of symmetry at $y = 0$. The domain for the radiation calculations is taken to be $(-20, 40) \times (0, 40) \times (0, 130)$, with domain boundaries taken to be symmetry boundaries or black surfaces at ambient temperature as appropriate. The computational mesh expands geometrically away from the origin with a total number of control volumes of $32 \times 24 \times 80$.

Figure 4 is a contour map of the temperature field on the plane of symmetry, showing the flame shape. In Fig. 5 two predictions of the external radiation field are compared with the measured heat flux at six locations. The radiative heat flux meters are arranged in a line at an angle of 20° to the wind direction, 1.5 m above ground level. The receivers are oriented in an attempt to capture the maximum radiative flux obtainable at a given point in space, by pointing their normals at the approximate flame centre. The accurate prediction of the flame structure is a nontrivial exercise. Using an integral model to specify the flame structure and a mixed grey gas model for the absorption coefficient introduces sources of error associated with the modelling assumptions in each of the submodels. These physical modelling errors and the experimental uncertainty present in any field scale experiment clouds the assessment of the suggested modifications to the original discrete transfer method. With this limitation in mind, the predicted heat flux distribution using Q_{Newt} and the recurrence relation (7) is in closer agreement with the measured data than Shah's original algorithm.

Although the different contributions to the error

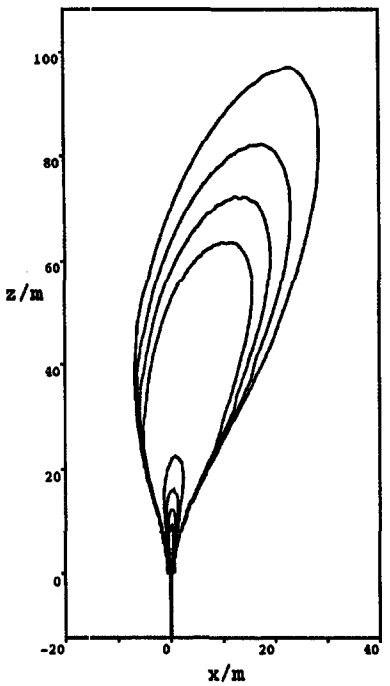

Fig. 4. Temperature field for the flare, $y = 0$. Contour values of 900, 1100, 1300 and 1500 K.

makes a detailed comparison between the two recurrence relations (2) and (7) difficult, an assessment of the rate of convergence of the two quadrature formulae Q_{Shah} and Q_{Newt} as the number of rays is increased can be made. Figure 6 shows the relative difference between the predicted heat flux at $x' = 30$ m and the ray converged value as a function of the number of rays, for the two quadrature formulae. Each line is generated by calculating the relative difference for four ray distributions and fitting a smooth interpolating polynomial. Each successively finer ray distribution is specified by halving $\Delta\phi$ and $\Delta\theta$. As can be seen in the figure the Q_{Newt} curve is within 4% of the ray converged value when 193 or

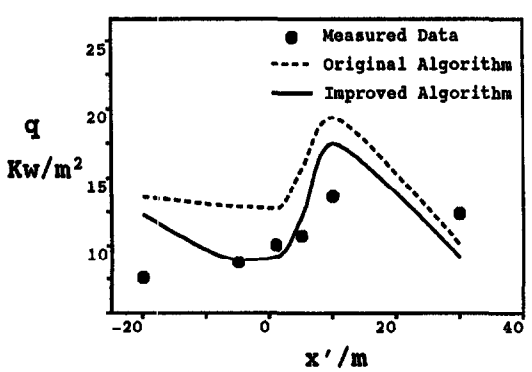

Fig. 5. Comparison of predicted fluxes with measured values for the flare. (a) Shah's original algorithm with 192 rays and (b) Q_{Newt} and recurrence relation (7) with 193 rays.

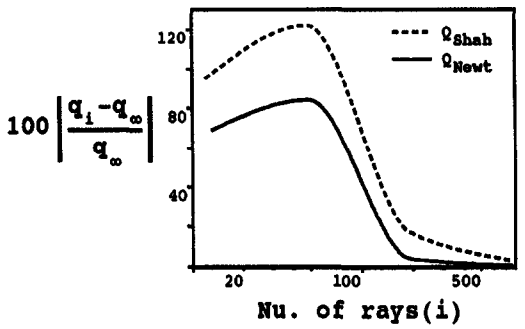

Fig. 6. Rate of convergence for predicted heat flux at $x' = 30$ m for the quadrature formulae Q_{Shah} and Q_{Newt}.

more rays are used, whereas Q_{Shah} requires 768 rays to achieve the same level of convergence.

5. COMPUTATIONAL EFFICIENCY OF THE DISCRETE TRANSFER METHOD

A final aspect of the discrete transfer method that warrants further investigation is the computational efficiency of the algorithm, when it is applied iteratively; that is when the walls are grey, the radiative source distribution is specified or the radiation model is coupled to a computational fluid dynamic solver. Returning to the 1D scenario (two infinite parallel surfaces) four iterations are required to satisfy the convergence criteria. Computer profiling the discrete transfer method algorithm on a Silicon Graphics Iris 4D/35 workstation to identify the computer intensive parts of the algorithm, it was found that nearly 70% of execution time was accumulated tracing rays through the domain. Note that once the hemispherical mesh is specified the direction of all rays is fixed. Hence it is possible to calculate the control volumes traversed, the distance travelled in each control volume and the walls impinged for each ray during the first iteration and store the information. For subsequent iterations the stored geometric information can be used rather than recalculated.

Implementing the discrete transfer method in this way for the 1D problem gives a speed-up coefficient of $S_p = 2.1$, where $S_p = t_{\text{cal}}/t_{\text{sto}}$, t_{cal} is the execution time for the algorithm with the ray trace calculated every iteration, and t_{sto} is the execution time for the algorithm when the ray trace is calculated once and stored. This, however, is not a good measure of improved performance as it is specific to this problem. A better measure is the speed-up coefficient for one iteration of the algorithm, which is $S_p = 3.5$. This is a good measure of improved performance as the once and for all calculation of the ray trace is a small overhead when many iterations of the discrete transfer method are performed, which is the case when used in conjunction with a computational fluid dynamic solver.

Application of the algorithm to a wide variety of problems on a number of computer systems indicates

the speed-up coefficient is insensitive to the number of rays and control volumes used but is sensitive to geometric complexity and the computer hardware employed. For rectangular enclosures and a variety of computer systems the speed-up coefficient for one iteration varied from 3.5 to 6.1.

The disadvantage of calculating the ray trace once and storing the information is that even for a modest number of rays and a coarse finite-difference grid this requires a large memory capacity. When Lockwood and Shah [7] formulated the discrete transfer method in its original implementation, one of its advantages over other models was its modest memory requirements as computer memory was expensive. Over the last decade computer technology has advanced such that memory now is an inexpensive component of a computer system making the 'once and for all' ray trace implementation feasible.

6. CONCLUSIONS

In this article the discrete transfer method of Lockwood and Shah [7] for calculating radiative heat transfer has been examined. Various aspects of the algorithm have been analysed and modifications suggested to improve the accuracy and computational performance. In particular, a number of quadrature formulae have been derived for calculating the incident flux distribution, and a more accurate representation of the temperature field has been harnessed in the calculation of intensity throughout the domain.

These modifications have been evaluated by comparing predicted heat fluxes with analytic and numerically accurate solutions to test problems as well as measured fluxes for a wind blown flare. The evaluation study shows that the modifications yield significant improvements over the numerical approximations formulated by Lockwood and Shah [7].

Acknowledgements—The author wishes to thank Geoff Cox and Suresh Kumar for stimulating his interest in radiative heat transfer. This paper is published by permission of British Gas Plc.

REFERENCES

1. F. C. Lockwood and W. M. G. Malalesekera, Fire computation: the 'flashover' phenomenon, *Proceedings of the Twenty second International Symposium on Combustion*, pp. 1319–1327. The Combustion Institute (1988).
2. K. Kuo, *Principles of Combustion*, Chap. 7. Wiley, New York (1986).
3. W. P. Jones and J. H. Whitelaw, Calculation methods for reacting turbulent flows: a review, *Combust. Flame* **48**, 1–26 (1982).
4. S. Kumar, A. K. Gupta and G. Cox, Effects of thermal radiation on the fluid dynamics of compartment fires, *Proceedings of the Third International Symposium on Fire Safety Science*, pp. 345–354. Hemisphere, New York (1991).
5. M. Fairweather, W. P. Jones and R. P. Lindstedt, Predictions of radiative transfer from a turbulent reacting jet in a cross-wind, *Combust. Flame* **89**, 45–63 (1992).
6. R. Siegel and J. R. Howell, *Thermal Radiation and Heat Transfer*. McGraw-Hill, New York (1972).
7. F. C. Lockwood and N. G. Shah, A new radiation solution method for incorporation in general combustion prediction procedures, *Proceedings of the Eighteenth International Symposium on Combustion*, pp. 1405–1413. The Combustion Institute (1981).
8. J. S. Truelove, Mixed grey gas model for flame radiation, AERE R 8494, UKAEA, Harwell, U.K. (1976).
9. W. L. Grosshandler, Radiation from non-homogeneous gases: a simplified approach, *Int. J. Heat Mass Transfer* **23**, 1447–1459 (1980).
10. P. Docherty and M. Fairweather, Predictions of radiative transfer from non-homogeneous combustion products using the discrete transfer method, *Combust. Flame* **71**, 79–87 (1988).
11. A. D. Gosman, F. C. Lockwood, I. E. Megahed and N. G. Shah, The prediction of the flow reaction and heat transfer in the combustion chamber of a glass furnace, *Proceedings of the Eighteenth Aerospace Science Meeting*, paper 80-0016, Pasadena (1980).
12. P. S. Cumber, S. Kumar and D. Smith, Evaluation of the discrete transfer method and its application to fire modelling, Eurotherm seminar No. 13: Fire modelling, UKAEA, Harwell June (1990).
13. N. G. Shah, New method of computation of radiant heat transfer in combustion chambers, Ph.D. Thesis, University of London (1979).
14. P. W. Guilbert, Comparison of Monte Carlo and discrete transfer method for modelling thermal radiation, AERE-R 13423, UKAEA, Harwell, U.K. (1989).
15. C. F. Gerald and P. O. Wheatley, *Applied Numerical Analysis* (3rd Edn), Chap. 4. Addison-Wesley, London (1984).
16. M. A. Heaslet and R. F. Warming, Radiative transport and wall temperature slip in an absorbing planar medium, *Int. J. Heat Mass Transfer* **8**, 979–994 (1965).
17. D. K. Cook, A one-dimensional integral model of turbulent jet diffusion, *Combust. Flame* **85**, 143–154 (1991).
18. D. K. Cook, An integral model of turbulent non-premixed jet flames in a cross-flow, *Proceedings of the Twenty Third International Symposium on Combustion*, pp. 653–660. The Combustion Institute (1990).
19. M. Caulfield, D. K. Cook, P. Docherty and M. Fairweather, An integral model of turbulent jets in a cross-flow *Part 2—II. Fires, Trans IChemE*, Part B **71**, 243–251 (1993).